ADVANCES IN ATMOSPHERIC SCIENCES, VOL. 34, JULY 2017, 805–815

• **Data Description Article** •

Two Ultraviolet Radiation Datasets that Cover China

Hui LIU[1,2], Bo HU*[1], Yuesi WANG[1], Guangren LIU[1], Liqin TANG[3], Dongsheng JI[1], Yongfei BAI, Weikai BAO, Xin CHEN, Yunming CHEN, Weixin DING, Xiaozeng HAN, Fei HE, Hui HUANG, Zhenying HUANG, Xinrong LI, Yan LI, Wenzhao LIU, Luxiang LIN, Zhu OUYANG, Boqiang QIN, Weijun SHEN, Yanjun SHEN, Hongxin SU, Changchun SONG, Bo SUN, Song SUN, Anzhi WANG, Genxu WANG, Huimin WANG, Silong WANG, Youshao WANG, Wenxue WEI, Ping XIE, Zongqiang XIE, Xiaoyuan YAN, Fanjiang ZENG, Fawei ZHANG, Yangjian ZHANG, Yiping ZHANG, Chengyi ZHAO, Wenzhi ZHAO, Xueyong ZHAO, Guoyi ZHOU, and Bo ZHU

[1]*State Key Laboratory of Atmospheric Boundary Layer Physics and Atmospheric Chemistry, Institute of Atmospheric Physics, Chinese Academy of Sciences, Beijing* 100029*, China*

[2]*Key Laboratory for Semi-Arid Climate Change, Ministry of Education, College of Atmospheric Sciences, Lanzhou University, Lanzhou* 730000*, China*

[3]*College of Atmospheric Sciences, Chengdu University of Information Technology, Chengdu* 610225*, China*

Note: Please refer to the Authors and Contributions section for other authors' details.

(Received 1 December 2016; revised 16 February 2017; accepted 14 March 2017)

ABSTRACT

Ultraviolet (UV) radiation has significant effects on ecosystems, environments, and human health, as well as atmospheric processes and climate change. Two ultraviolet radiation datasets are described in this paper. One contains hourly observations of UV radiation measured at 40 Chinese Ecosystem Research Network stations from 2005 to 2015. CUV3 broadband radiometers were used to observe the UV radiation, with an accuracy of 5%, which meets the World Meteorology Organization's measurement standards. The extremum method was used to control the quality of the measured datasets. The other dataset contains daily cumulative UV radiation estimates that were calculated using an all-sky estimation model combined with a hybrid model. The reconstructed daily UV radiation data span from 1961 to 2014. The mean absolute bias error and root-mean-square error are smaller than 30% at most stations, and most of the mean bias error values are negative, which indicates underestimation of the UV radiation intensity. These datasets can improve our basic knowledge of the spatial and temporal variations in UV radiation. Additionally, these datasets can be used in studies of potential ozone formation and atmospheric oxidation, as well as simulations of ecological processes.

Key words: ultraviolet radiation, observation, hybrid model, reconstruction, China

Citation: Liu, H., and Coauthors, 2017: Two ultraviolet radiation datasets that cover China. *Adv. Atmos. Sci.*, **34**(7), 805–815, doi: 10.1007/s00376-017-6293-1.

Dataset Profile

Dataset title	UV radiation datasets covering China
Time range	Observed hourly UV radiation: 2005–15 Reconstructed daily UV radiation: 1961–2014
Geographical scope	China's mainland
Data format	".xlsx" for the observed data; ".txt" for the reconstructed data
Data volume	80 MB for the hourly observations of UV radiation; 60 MB for the reconstructed daily UV radiation
Data service system	http://www.dx.doi.org/10.11922/sciencedb.332 DOI: 10.11922/sciencedb.332

(to be continued)

* Corresponding author: Bo HU
E-mail: hub@post.iap.ac.cn

(Continued)

Dataset Profile	
Sources of funding	Strategic Priority Research Program of the Chinese Academy of Sciences (Grant No. XDB05020402) National Basic Research Program (Grant No. 41275165); Science and Technology Service Network Project of the Chinese Academy of Sciences (Grant No. KFJ-SW-STS-168)
Dataset composition	The dataset consists of two compressed files, with the file names "observed uv radiation.zip" and "reconstructed uv radiation.zip". 1. The file "observed uv radiation.zip" contains the in situ–measured UV radiation dataset and comprises 40 Excel worksheets. Each file contains the data collected at a single station. 2. The file "reconstructed uv radiation.zip" contains the reconstructed UV radiation dataset, which consists of 725 .txt files. The file named "station information.txt" contains information on the site locations, and the other 724 file names correspond to the station codes.

1. Introduction

Although the ultraviolet (UV) solar spectrum contributes only approximately 8.0% of the entire solar radiation at the top of the atmosphere (Gueymard, 2004), it is vital for ecosystems and the environment (Williamson et al., 2014), human health and climate change (Ferrero et al., 2006; Thomas et al., 2012). UV radiation has gradually become one of the major topics investigated in current studies, especially since the discovery of the ozone hole. It is an indicator of the amount of ozone that will form. UV radiation can inhibit plant photosynthesis by destroying leaves, which subsequently affects the balance of ecosystems. The absorption cross section of a gas multiplied by the amount of UV radiation gives the rate of photolysis, which determines atmospheric oxidation, affects photochemical reactions and produces secondary pollutants in the near-surface layer. Moreover, excess UV radiation may induce sunburn, skin cancer, and eye cataracts. In the stratosphere, the absorption of solar UV radiation by ozone counteracts the effect of radiative cooling caused by increases in carbon dioxide and water vapor.

The amount of UV radiation that penetrates to the surface depends mainly on the solar zenith angle, the presence of clouds, aerosols, ozone, and surface reflectivity (Bais et al., 1993; Arola, 2003; Bernhard et al., 2007; Kerr and Fioletov, 2008). The interactions between UV radiation and these factors are complex and not yet fully understood. den Outer et al. (2010) reconstructed UV radiation back to 1960 in Europe and found that UV levels have gradually increased over the last four decades, particularly since the 1980s. With regard to the period from 1980 to 2006, approximately two-thirds of the increase in UV radiation can be attributed to a decline in cloudiness or aerosol optical depth (AOD) and one-third can be attributed to reductions in ozone. Wei et al. (2006) analyzed the long-term changes in ozone and noontime erythemal UV radiation from 1978 to 2011 using Total Ozone Mapping Spectrometer data products. They found that, in the eastern and southern parts of China, the ozone layer is not the main reason for the trend in UV irradiance; rainfall and the related cloud variations have significant correlations with UV radiation in these regions, and approximately 40%–70% of the variability in UV radiation there can be explained by precipitation change. On the other hand, in the western and northern parts of China, variations in ozone can explain approximately 30%–70% of the variations in UV radiation. Measurements from October 2004 to September 2006 at Xianghe Station were used to analyze the relationships between UV radiation and meteorological factors (Xia et al., 2008). It was found that aerosols can cause a reduction of approximately 0.0091 in F_{UV} (the ratio of UV radiation to the amount of solar radiation reaching the surface) per unit increase in AOD (500 nm) for precipitable water vapor content within a range of 1.5–2.0 cm. Additionally, an increase of 17% in F_{UV} resulted from an increase of 1.0 cm in the precipitable water vapor content; F_{UV} increased by 20% when the ground was covered with snow. It was difficult to quantify the role of each factor because the contribution of each factor is different in different time periods and regions. Thus, accurate measurements of UV radiation and the main factors controlling its levels at the surface of the Earth are of great importance for achieving better understanding of the interactions between UV radiation, ozone, aerosols, clouds and surface reflectivity (Schwander et al., 1997; Mayer and Kylling, 2005).

Unfortunately, as UV radiation is not a routinely measured parameter, in situ measurements of UV radiation are very scarce, especially in China. The network for observing UV radiation in China started very late. In the early 1990s, the UV radiation observation system of Brewer was first built in the background stations of Waliguan and Zhongshan for long-term continuous observations. Additionally, domestic scientific researchers have established UV radiation observation stations at a few, widely distributed locations. Although many characteristics of UV radiation have been obtained, the time scale is very short, and the results are local and not regionally representative. Therefore, it is important to carry out research on the measurement of UV radiation on a national scale.

The aim of this paper is to introduce two datasets describing UV radiation. One contains hourly observations of UV radiation from 40 Chinese Ecosystem Research Network (CERN) stations in China, and the other contains reconstructed daily UV radiation amounts at 724 China Meteorological Administration (CMA) stations. The latter used

a UV estimation model combined with a hybrid model that was proposed and then improved by Yang et al. (2001, 2006). Basic information on the observed and reconstructed data is provided in section 2. A sample description of the datasets is presented in section 3, and some applications of the data are described in section 4.

2. Basic data information

Basic information on the dataset is presented in the data profile table, including the time range and geographical scope that it covers, the dataset's composition, and so on. In sections 2.1 and 2.2, detailed information on the observed and reconstructed properties of the data are described.

2.1. *Collection of the observed UV radiation data*

The UV radiation data were obtained from a national-scale network, CERN, which was the first standard network established to measure solar radiation for investigating the radiation budget and its spatial and temporal variations over China. CERN consists of 40 stations that provide in situ measurements of UV radiation, covering almost all typical ecosystems. Two stations are in grassland ecosystems, there is one urban station, three for bays, two for lakes, six for deserts, fifteen for agriculture, ten for forests, and one for marshland. The spatial distribution of the 40 CERN stations in China is shown in Fig. 1, and the geographical locations, altitudes and ecosystem types of the stations are provided in Table 1. The urban station, in Beijing, which is located at the Institute of Atmospheric Physics of the Chinese Academy of Sciences, is the center of data collection, quality control and instrument calibration for the entire radiation observation system.

CUV3 broadband radiometers (Kipp & Zonen, The Netherlands), which have an accuracy of 5%, have been installed at all CERN stations to make observations of UV radiation (290–400 nm). This level of accuracy meets the World Meteorological Organization's (WMO) measurement standards. UV pyranometers are calibrated using standard lamps with a known spectroradiometer, and this calibration system is at the forefront of UV radiation research in China. A spectrometer measures a standard lamp spectral irradiance and then retrieves the spectral sensitivity under standard lamp conditions (K_c). Using the same method, the spectral sensitivity under sunshine conditions (K_s) can be deduced. The K_c is considered equal to K_s in narrow wavebands. For each narrow waveband, K_c can be obtained by using the lamp spectral irradiance, and the spectroradiometer can then be used to measure solar irradiance. The UV radiation can be derived by integrating the solar spectral irradiance between 290 and 400 nm. At the same time, the calibrated UV pyranometers measure the response voltage. All CUV3 pyranometers are calibrated and inter-compared at the beginning and the end of data collection to ensure the accuracy of the calibration. Daily checks are made to ensure that the radiometers are free of dirt and positioned horizontally to guarantee the data quality. M520 (Vaisala) data collectors are used to collect the data. All radiation data are recorded at 1-min intervals, and hourly values are derived from the 1-min values through integration.

2.2. *Quality control of the observed UV radiation*

UV radiation data quality controls are conducted on two aspects. One of these aspects is the observation system, and the other involves a quality assessment of the UV radiation measurement data.

In terms of the first aspect, all radiation sensors and data collectors used at the CERN stations meet the WMO's standards for radiation observations. The UV pyranometers at individual stations are calibrated monthly against reference instruments that have been calibrated against regional reference instruments, which in turn are calibrated against Chinese reference instruments every two years. Data that are missing due

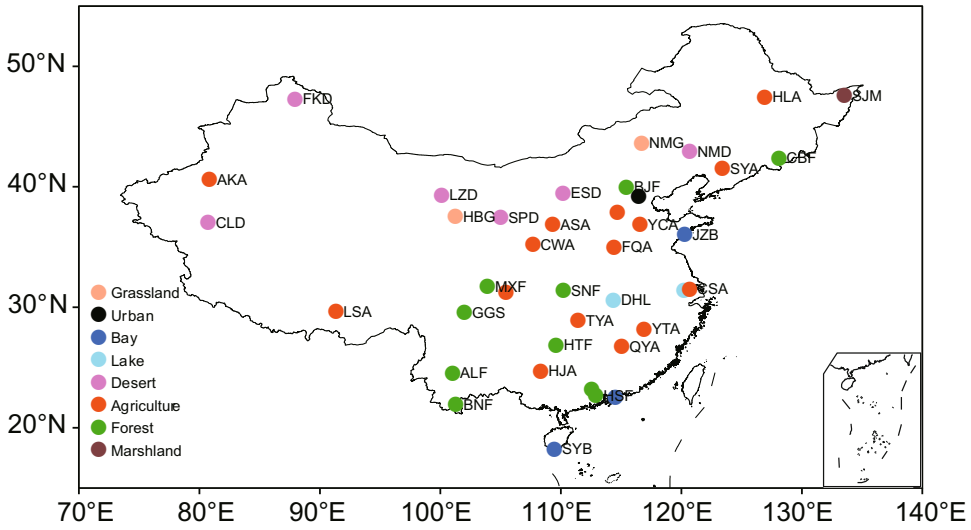

Fig. 1. Spatial distribution of the CERN radiation stations.

Table 1. Information on the dataset's sites belonging to the CERN network.

Station code	Station name	Longitude (E)	Latitude (N)	Elevation (m)	Ecological type	Effective data magnitude
AKA	Akesu	80.83	40.62	1028	Agriculture	24613
ASA	Ansai	109.32	36.86	1189	Agriculture	38600
CSA	Changshu	120.68	31.53	1.3	Agriculture	36444
CWA	Changwu	107.67	35.2	1120	Agriculture	32016
FQA	Fengqiu	114.4	35	67.5	Agriculture	38651
HJA	Huanjiang	108.32	24.73	279	Agriculture	24287
HLA	Hailun	126.92	47.45	240	Agriculture	39259
LCA	Luancheng	114.69	37.89	50.1	Agriculture	37576
LSA	Lhasa	91.33	29.67	3688	Agriculture	40750
QYA	Qianyanzhou	115.05	26.73	100	Agriculture	39385
SYA	Shenyang	123.4	41.52	31	Agriculture	40025
TYA	Taoyuan	111.43	28.92	77.5	Agriculture	38719
YCA	Yucheng	116.57	36.87	21	Agriculture	40383
YGA	Yanting	105.45	31.27	460	Agriculture	37780
YTA	Yingtan	116.92	28.2	35.6	Agriculture	39255
DYB	Daya Bay	114.52	22.55	21	Bay	37557
JZB	Jiaozhou Bay	120.27	36.05	15	Bay	35578
SYB	Sanya	109.48	18.22	3	Bay	39715
CLD	Cele	80.72	37.02	1371	Desert	42058
ESD	Eerduosi	110.18	39.48	1290	Desert	36442
FKD	Fukang	87.93	47.29	460	Desert	39112
LZD	Linze	100.12	39.33	1120	Desert	43042
NMD	Naiman	120.7	42.93	358	Desert	39145
SPD	Shapoutou	105	37.47	1357	Desert	40331
ALF	Ailao Mountain	101.02	24.53	2450	Forest	40079
BJF	Beijing forest	115.43	39.97	1150	Forest	31660
BNF	Xishuangbanna	101.27	21.92	570	Forest	39375
CBF	Changbai Mountain	128.1	42.4	736	Forest	40851
DHF	Dinghu Mountain	112.55	23.17	1000.3	Forest	40941
GGF	Gongga Mountain	102	29.58	3000	Forest	38885
HSF	He Mountain	112.9	22.68	80	Forest	38299
HTF	Huitong	109.6	26.85	305	Forest	37237
MXF	Maoxian	103.9	31.7	1816	Forest	37909
SNF	Shennongjia	110.22	31.38	1290	Forest	27536
HBG	Haibei	101.25	37.53	3230	Grassland	32841
NMG	Inner Mongolia	116.7	43.63	1187	Grassland	37483
DHL	Lake Dong	114.35	30.62	18	Lake	37322
THL	Lake Tai	120.22	31.42	10	Lake	38864
SJM	Sanjiang	133.52	47.58	56.2	Marshland	37561
ASC	Beijing	116.46	39.22	53	Urban	38797

to human error or sensor failure are represented by 32766. As there is no UV radiation at night, the UV radiation data are blank in the Excel cells for when the solar elevation angle is negative.

The quality assessment for the UV radiation measurement data is primarily based on three principles. First, considering the cosine response, the UV radiation data are replaced with 9999 when the solar elevation angle is less than 5° (Huang et al., 2011). Second, each observed hourly UV radiation value should be less than the hourly extraterrestrial UV radiation at the top of the atmosphere at the same geographical location; otherwise, it is flagged as questionable data and replaced with 9999. The extraterrestrial UV radiation (UV_{ext}), is calculated using Eq. (1), which was proposed by Foyo-Moreno et al. (1999):

$$UV_{ext} = I_{suv}\left(\frac{12}{\pi\rho^2}\right)\int_{w_1}^{w_2}\sin(\alpha)\mathrm{d}w\,, \quad (1)$$

where I_{suv} is the ultraviolet spectral irradiance and is equal to 78 W m^{-2}; ρ is the distance correction factor between the Sun and Earth; α is the solar zenith angle; and w is the time angle. Third, the ratio of UV radiation to the global solar radiation (R_s) should be limited to values between 0.02 and 0.08; otherwise, the data are replaced with 9999 (Hu et al.,

2007). All the quality control procedures were carried out using the FORTRAN 90 program. The values in the last column of Table 1 are the effective data quantities after quality control.

2.3. *Development of the reconstructed UV radiation data*

The UV radiation observation system in China started relatively late compared to similar systems elsewhere around the world. Most of the observed UV datasets described above begin in 2005, and the observation sites are very sparse. To obtain high spatial resolution and long records of historical UV radiation data, either empirical and semi-physical methods or satellite inversion algorithms can be used. In this study, daily UV radiation datasets for the period before the use of instrumentation were obtained from solar radiation measurements through an all-sky UV estimation model. However, in the CMA radiation network, only around 120 sites can provide daily solar radiation. Moreover, due to the retrofitting of many of the radiation instruments before 1993, the accuracy of the observed solar radiation data was relatively low during that period (Tang et al., 2011). Instead of using these data, solar radiation amounts reconstructed with a hybrid model were used to calculate the UV radiation.

2.3.1. *Reconstructing solar radiation using a hybrid model*

The hybrid model put forward and improved by Yang et al. (2001, 2006) was applied to estimate solar radiation using the AOD and total column ozone measurements retrieved from satellite data and routine meteorological observations obtained from the CMA. The details of this hybrid model have been described by Yang et al. (2006), so only a brief description is given here. Physical processes, such as Rayleigh scattering, aerosol extinction, ozone absorption, water vapor absorption, permanent gas absorption, and the effects of clouds, which are represented by the transmittance functions τ_r, τ_a, τ_{oz}, τ_w and τ_c, respectively, are considered, and the simplicity of the Ångström correlation is also maintained in the hybrid radiative transfer model. The solar beam radiative transmittance (τ_d) and the solar diffuse radiative transmittance (τ_d) under clear skies can be calculated using Eqs. (2) and (3):

$$\tau_b = \tau_r \tau_a \tau_{oz} \tau_w \tau_g \; ; \tag{2}$$

$$\tau_d = 0.5[\tau_{oz} \tau_g \tau_w (1 - \tau_a \tau_r)] \; . \tag{3}$$

Solar radiation reaching the surface of the Earth can be obtained using the following equation:

$$R_s = \tau_c \int_{\Delta t=24} (\tau_b + \tau_d) R_0 \mathrm{d}t \; , \tag{4}$$

where R_0 is the solar radiation at the top of the atmosphere, t is time, and Δt is the integration period.

More detail on the methods for calculating τ_r, τ_a, τ_{oz}, τ_g and τ_c can be found in the paper by Yang et al. (2006). The data required by the model as the input, including surface pressure, surface relative humidity, air temperature, and sunshine duration, which were obtained from routine observations at 724 weather stations (Fig. 2) with specified latitudes and longitudes, underwent quality control by the CMA. Other input values, such as the AOD and total column ozone at the 724 stations, were interpolated from satellite retrievals. The column ozone concentrations were obtained from the Solar Backscatter Ultraviolet Merged Ozone Data Set, Version 8.6 (http://acd-ext.gsfc.nasa.gov/Data_services/merged/index.html). The AOD was obtained from a MODIS data product (MOD08-M3, level 3, Collection 5.1) (http://ladsweb.nascom.nasa.gov/data/search.html) with a spatial resolution of $1^\circ \times 1^\circ$. As no AOD data were available before 2000, and no ozone data before 1970, climatic mean AOD and ozone values were used in the hybrid model.

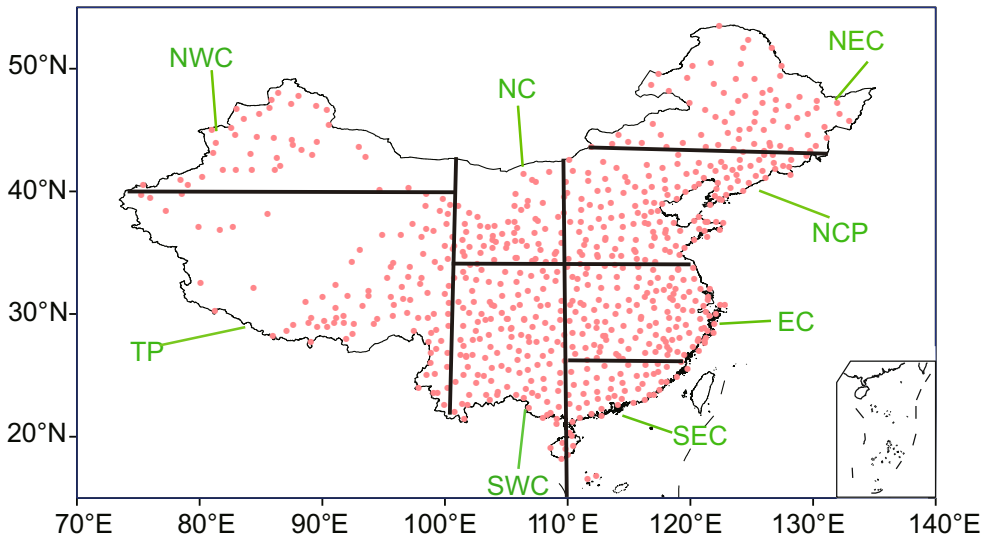

Fig. 2. Map of the CMA sites that contributed data to the reconstruction of daily solar radiation values.

All the calculations involved in the hybrid model were conducted using the FORTRAN 90 program. Using this hybrid model, daily solar radiation values from 1961 to 2014 were obtained and could be used to reconstruct the daily UV radiation.

2.3.2. *Reconstructing UV radiation by combining the hybrid model results with an all-sky UV estimation model*

As UV radiation is highly correlated with solar radiation, most published experimental results use measured solar radiation to calculate UV radiation by considering the ratio of UV radiation to solar radiation as an empirical constant (Calbó et al., 2005; Podstawczynska, 2010). Long and Ackerman (2000) used a power law equation to describe the dependence of solar radiation on the cosine of the solar zenith angle under clear-sky conditions. The clearness index (K_t) is defined as the ratio of the solar irradiance reaching the surface of the Earth to the extraterrestrial solar irradiance, and it provides a general indication of scattering and absorption processes due to aerosols, gases, clouds, etc. Earlier studies of the effects of K_t and the solar zenith angle on UV radiation have been analyzed and confirmed under different sky conditions (Hu et al., 2010; Wang et al., 2013; Liu et al., 2016). To develop the estimation model, the entire hourly dataset from Lhasa Station under all weather conditions was studied. Figure 3a displays the UV radiation plotted against the cosine of the solar zenith angle (μ). Different colors represent different K_t values. For a given specific K_t interval, it is recommended that the relationship between UV radiation and the cosine of the solar zenith angle is calculated with the following power law equation:

$$\mathrm{UV} = \mathrm{UV}_0 \mu^e \,, \tag{5}$$

where UV_0 indicates the UV radiation for one unit of μ, and e determines how UV varies with μ. Unfortunately, it is not straightforward to obtain direct measurements of UV_0, as that requires the solar zenith angle to be zero.

K_t was first allocated as 0.03, with a step size of 0.01. The relationship between UV and μ was fitted using the power law equation [Eq. (5)] within each specific K_t interval. The relationship between UV_0 and K_t was then analyzed (Fig. 3b). The dependence of UV_0 on K_t is described by Eq. (6):

$$\mathrm{UV}_0 = a + bK_t + cK_t^2 + dK_t^3 \,, \tag{6}$$

where the units of a, b, c and d are W m^{-2}.

The long-term observed daily values of R_s could be easily obtained from the hybrid model, but long-term hourly values of R_s were not obtainable. Therefore, Eqs. (5) and (6) were modified to calculate daily UV radiation amounts using the daily values of R_s, as follows:

$$\mathrm{UV}_{\mathrm{daily}} = (A + B\overline{K}_t + C\overline{K}_t^2 + D\overline{K}_t^3)\bar{\mu}^E t_{\mathrm{d}} \,, \tag{7}$$

where $\mathrm{UV}_{\mathrm{daily}}$ is the daily amount of UV radiation; the units of this quantity are MJ (m^2 d)$^{-1}$. $\overline{K}_t$ is the ratio of daily R_s to daily extraterrestrial solar irradiance; $\bar{\mu}$ is the average of the cosine of the solar zenith angle from sunrise to sunset; t_{d} is the daily sunshine duration (hours); and A, B, C, D and E are parameters that differ between climatic zones. Therefore, China was divided into eight climatic zones, and the UV radiation data were reconstructed using the corresponding values of the parameters A to E, given in Table 2, and combined with the solar radiation estimates obtained from the hybrid model.

Table 2. UV radiation estimation models in different climate regions.

Typical station	Subregion	A	B	C	D	E
FKD	NWC	−0.001	0.33	−0.25	0.14	1.22
LSA	TP	0.038	0.08	0.36	−0.28	1.31
SPD	NC	0.000	0.36	−0.40	0.33	1.41
YGA	SWC	−0.004	0.41	−0.57	0.49	1.36
HLA	NEC	0.003	0.30	−0.24	0.16	1.27
BJF	NCP	0.003	0.26	−0.24	0.19	0.95
DHL	EC	0.000	0.39	−0.48	0.42	1.56
DHF	SEC	−0.002	0.36	−0.38	0.29	1.37

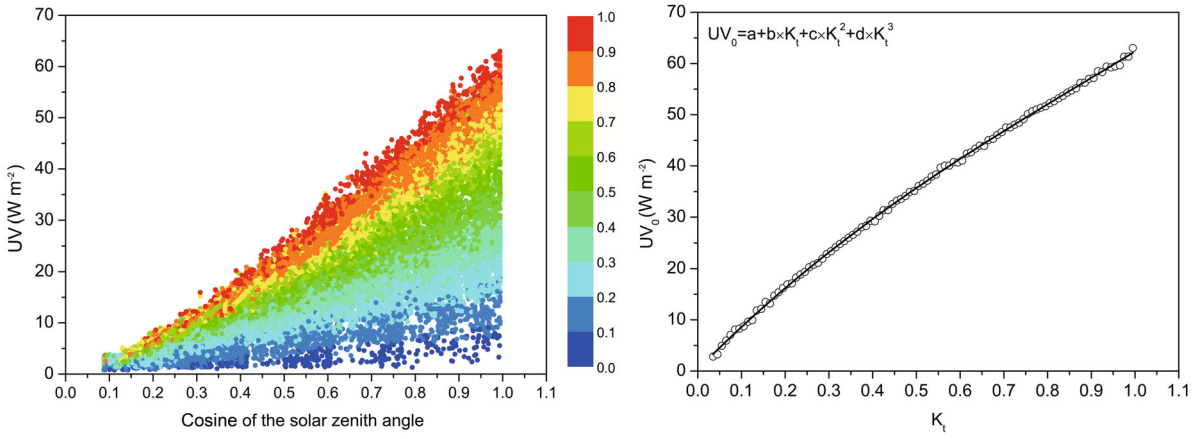

Fig. 3. The effects of K_t and μ on UV radiation at Lhasa (left) and a scatter plot showing UV_0 and K_t (right).

2.3.3. *Validation of the reconstructed UV radiation estimates*

To validate the accuracy of the UV radiation reconstruction model, the UV radiation amounts measured in situ at 40 CERN stations from 2005 to 2014 were chosen for comparison with the reconstructed UV radiation data obtained by applying the hybrid model and an all-sky UV estimation model to the nearest CMA station. Statistical estimators, such as the correlation coefficient (R), the mean bias error (MBE), the mean absolute bias error (MABE), and the root-mean-square error (RMSE) were used as benchmarks for the radiation products. These metrics are defined as follows:

$$R = \frac{\sum_{i=1}^{i=N}(E_i - E_{\text{ave}})(M_i - M_{\text{ave}})}{\sqrt{\sum_{i=1}^{i=N}(E_i - E_{\text{ave}})^2 \cdot \sum_{i=1}^{i=N}(M_i - M_{\text{ave}})^2}}; \quad (8)$$

$$\text{MBE} = \frac{100}{M_{\text{ave}}}\left(\frac{\sum_{i=1}^{i=N}(E_i - M_i)}{N}\right); \quad (9)$$

$$\text{MABE} = \frac{100}{M_{\text{ave}}}\left(\frac{\sum_{i=1}^{i=N}|E_i - M_i|}{N}\right); \quad (10)$$

$$\text{RMSE} = \frac{100}{M_{\text{ave}}}\left(\frac{\sum_{i=1}^{i=N}(E_i - M_i)^2}{N}\right)^{0.5}. \quad (11)$$

Here, E_i is the estimated value (ith number), M_i is the measured value, E_{ave} is the average of the estimated values, M_{ave} is the average of the measured values, and N is the number of observations.

Table 3 shows the four statistical parameters calculated using the CERN-observed UV radiation and the calculated UV radiation at the nearest CMA stations. The correlation coefficient is larger than 0.8 for all stations except BNF and MXF. The MBE values are negative at 35 of the stations, which indicates that the reconstructed UV radiation values represent slight underestimates compared with the observations. Only MXF and THL have MABE values larger than 25% and RMSE values larger than 30%. All of the statistical results show that the reconstructed UV radiation values are reliable.

3. Sample description of the dataset

3.1. *Sample description of the observed UV radiation values*

The dataset, which contains UV radiation values measured in situ, is composed of 40 files. The format of the file names is "ABC.xlsx", where AB represents the station code, and C represents the type of ecosystem surrounding the station. All the corresponding information can be found in Table 1. Beijing Station is chosen as an example for describing the organization of the data (Table 4). Blank spaces in the last column indicate that the solar elevation is less than 0°, and there are no effective radiation data; 32766 represents a missing measurement caused by human error or sensor failure; and 9999 indicates that the UV radiation data do not satisfy the quality control principles described in section 2.2. The diurnal variation of UV radiation on 9 July 2015 and the annual average diurnal variation in UV radiation for 2015 at Beijing Station are presented in Fig. 4. The measured value of UV

Table 3. Statistics regarding the relationship between the CERN-observed UV radiation amounts and the UV radiation amounts calculated for the nearest CMA stations. The bold numbers indicate that MXF and THL have larger statistical results.

CERN station code	CMA station code	R^2	MBE (%)	MABE (%)	RMSE (%)
AKA	51628	0.88	−8.01	19.14	22.24
ALF	56856	0.83	−3.37	15.37	18.2
ASA	53845	0.93	−2.16	12.9	15.42
BJC	54518	0.95	5.81	13.26	15.45
BJF	54405	0.97	7.21	11.1	12.8
BNF	56959	0.77	−7.51	14.41	16.96
CBF	54285	0.92	−3.92	12.78	15.79
CLD	51828	0.9	−6.44	13.64	15.82
CSA	58259	0.91	−10.78	18.22	21.28
CWA	53929	0.9	0.33	16.49	19.13
DHF	59278	0.87	−8.47	18.59	21.5
DHL	57494	0.89	−11.71	21.18	24.4
DYB	59493	0.84	−12.29	19.67	22.69
ESD	53545	0.91	−11.7	16.44	18.7
FKD	51076	0.94	−10.87	16.72	19.41
FQA	57091	0.9	−16.15	22.05	25.3
GGS	56374	0.87	−6.69	15.11	17.9
HBG	52765	0.91	−7.79	13.26	16.03
HJA	59023	0.92	−2.13	15.9	18.52
HLA	50756	0.94	−6.19	13.17	15.94
HSF	59478	0.87	−5.68	15.64	18.27
HTF	57745	0.91	−1.87	21.59	24.84
JZB	54857	0.9	−6.33	14.42	17.69
LCA	53698	0.93	3.23	14.63	17.21
LSA	55591	0.81	−10.12	14.45	16.45
LZD	52546	0.93	−8.85	13.47	15.65
MXF	56188	0.75	−15.88	**26.6**	**30.56**
NMD	54226	0.93	−5.48	12.02	15.08
NMG	54102	0.89	−11.21	16.66	19.21
QYA	57799	0.89	−6.84	22.82	26.09
SJM	50788	0.91	−11.3	19.44	22.75
SNF	57355	0.91	−4.21	18.21	20.97
SPD	53704	0.9	−10.64	15.93	18.59
SYA	54342	0.93	−0.72	12.45	15.23
SYB	59948	0.85	−16.77	19.73	21.95
THL	58358	0.78	−20.07	**31.15**	**36.01**
TYA	57662	0.89	−7.23	22.1	25.61
YCA	54715	0.91	−1.44	14.03	16.79
YGA	57306	0.91	−4.11	17.56	20.58
YTA	58626	0.87	−11.6	24.93	28.3

Table 4. Observed UV radiation data at the Beijing CERN station on 9 July 2015. 32766 represents a missing measurement caused by human error or sensor failure, and 9999 indicates that the UV radiation data do not satisfy the quality control principles described in section 2.2.

Year	Month	Day	Local time (hour)	UV radiation (W m^{-2})
2015	7	9	0	—
2015	7	9	1	—
2015	7	9	2	—
2015	7	9	3	—
2015	7	9	4	—
2015	7	9	5	9999
2015	7	9	6	2.8
2015	7	9	7	6.2
2015	7	9	8	10.4
2015	7	9	9	15.7
2015	7	9	10	20.6
2015	7	9	11	25.7
2015	7	9	12	27.7
2015	7	9	13	27.5
2015	7	9	14	32766
2015	7	9	15	20.5
2015	7	9	16	15.2
2015	7	9	17	8.4
2015	7	9	18	3.9
2015	7	9	19	9999
2015	7	9	20	—
2015	7	9	21	—
2015	7	9	22	—
2015	7	9	23	—

radiation corresponding to 1400 LST 9 July 2015 is absent. The distribution of annual mean UV radiation in 2015 is shown in Fig. 5.

3.2. *Sample description of the reconstructed UV radiation*

The reconstructed UV radiation dataset comprises 725 files. The file named "station information.txt" contains information on each site's location and consists of three columns that contain the station codes, as well as their longitudes and latitudes, respectively. The file names of the other 724 files correspond to the five-digit station codes. Data collected during July 2014 at station 54511 (Beijing) are chosen as an example to describe the organization of the data (Table 5).

Table 5. Reconstructed UV radiation data at the Beijing CERN station in July 2014.

Year	Month	Day	UV radiation [MJ (m^2 d)$^{-1}$]
2014	7	1	0.308
2014	7	2	0.306
2014	7	3	0.343
2014	7	4	0.404
2014	7	5	0.646
2014	7	6	0.304
2014	7	7	0.303
2014	7	8	0.628
2014	7	9	0.571
2014	7	10	0.891
2014	7	11	0.855
2014	7	12	0.915
2014	7	13	0.847
2014	7	14	0.834
2014	7	15	0.802
2014	7	16	0.461
2014	7	17	0.298
2014	7	18	0.637
2014	7	19	0.813
2014	7	20	0.838
2014	7	21	0.53
2014	7	22	0.299
2014	7	23	0.296
2014	7	24	0.366
2014	7	25	0.832
2014	7	26	0.835
2014	7	27	0.83
2014	7	28	0.793
2014	7	29	0.625
2014	7	30	0.287
2014	7	31	0.408

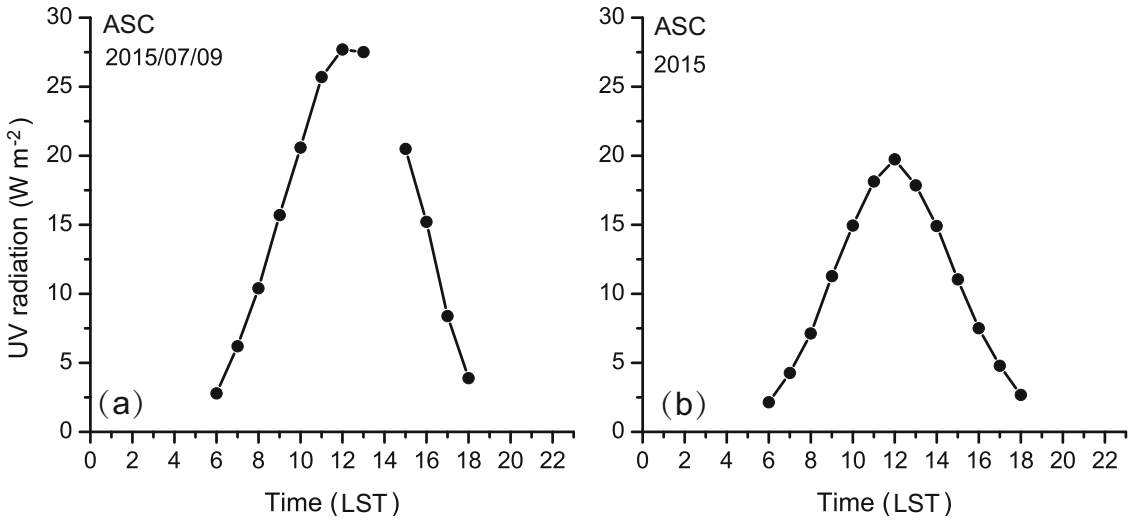

Fig. 4. Diurnal variation in UV radiation at Beijing Station: (a) 9 July 2015; (b) annual average for 2015.

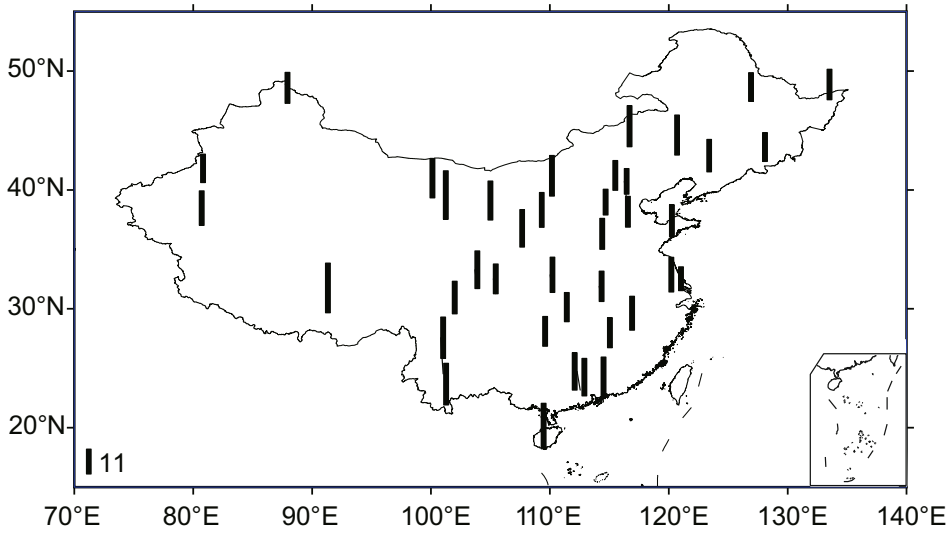

Fig. 5. Spatial distribution of observed UV radiation at the CERN stations in 2015 (units: W m^{-2}).

The four columns represent the year, month, day and reconstructed daily UV radiation, respectively. The annual variation in reconstructed UV radiation in 2014 at station 54511 is shown in Fig. 6. For some stations, 32766 may appear in the fourth column, which represents the absence of reconstructed data. The distribution of annual mean reconstructed UV radiation in 2014 is presented in Fig. 7. This distribution is similar to the distributions of photosynthetically active radiation and surface solar radiation reconstructed by Tang et al. (2013a, 2013b).

4. Data applications

UV radiation may have serious effects on public health, such as skin cancer, accelerated aging of the skin, cataracts and other eye diseases. It can also reduce the ability to resist infectious diseases. Increased UV radiation may reduce

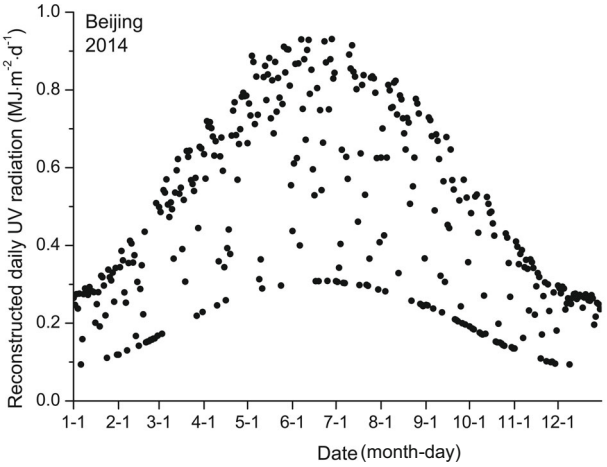

Fig. 6. Annual variation in the reconstructed UV radiation in 2014 at Beijing Station.

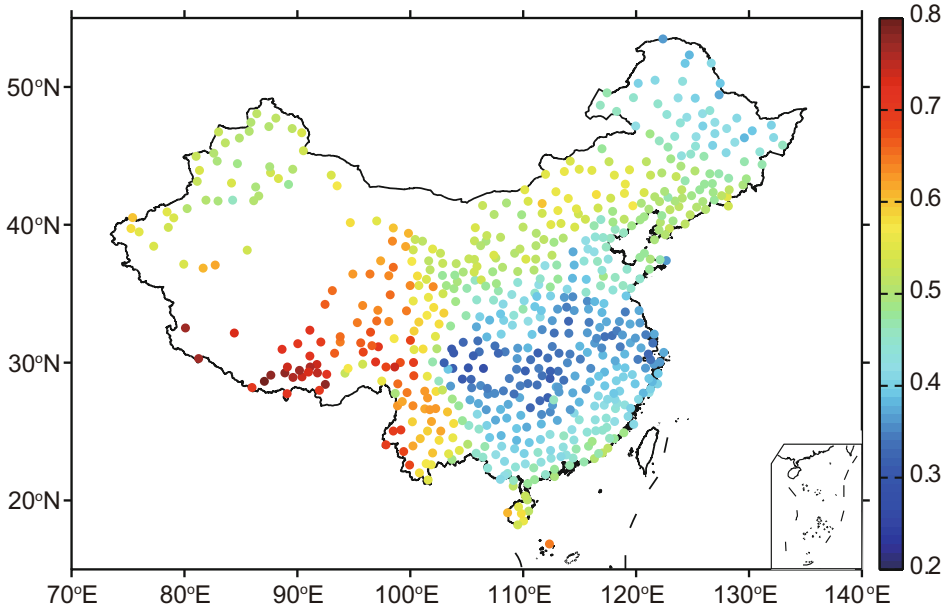

Fig. 7. Spatial distribution of reconstructed UV radiation at the CMA stations in 2014 [units: MJ (m^2 d)$^{-1}$].

growth in several plant species or diminish photosynthetic activity. UV radiation also plays important roles in atmospheric chemistry processes, such as the production of dimethyl sulfide, hydroxyl radicals, tropospheric ozone and ozone precursors. Thus, UV radiation datasets are essential in a wide range of fields, including cancer research, ecology, tropospheric chemistry, agriculture and climate science.

The two UV radiation datasets described in this paper have the potential to improve our basic knowledge of the distribution of UV radiation over large temporal and spatial scales, which should contribute substantially to engineering applications in China and provide a scientific basis for sustainable energy and atmospheric environmental protection. Moreover, these datasets contain scientific data that support biological studies, ecological process simulations, and studies of atmosphere–land surface interactions. The datasets have been archived in the Science Data Bank (http://www.dx.doi.org/10.11922/sciencedb.332).

Acknowledgements. We thank CERN for providing the radiation observations. The global solar radiation data and meteorological elements used in this study were obtained from the CMA, which is highly appreciated by the authors. We also gratefully acknowledge the MODIS Science Team for providing the AOD dataset and the NASA/GSFC Ozone Processing Team for supplying the ozone data.

Authors and contributions

Hui LIU: data processing and paper writing;
Bo HU: data quality control;
Guangren LIU: data quality control;
Yuesi WANG: observation network design;
Liqin TANG: paper writing;
Dongsheng JI: paper editing;

In addition, many other staff members also contributed to the data observation and quality control, as follows:

Yongfei BAI, Zhenying HUANG, Hongxin SU, and Zongqiang XIE, the Institute of Botany, Chinese Academy of Sciences;

Weikai BAO, Chengdu Institute of Biology, Chinese Academy of Sciences;

Xin CHEN, Anzhi WANG and Silong WANG, the Institute of Applied Ecology, Chinese Academy of Sciences;

Yunming CHEN and Wenzhao LIU, the Institute of Soil and Water Conservation, Chinese Academy of Sciences;

Weixin DING, Bo SUN and Xiaoyuan YAN, the Institute of Soil Science, Chinese Academy of Sciences;

Xiaozeng HAN and Changchun SONG, the Northeast Institute of Geography and Agroecology, Chinese Academy of Sciences;

Fei HE and Wenxue WEI, the Institute of Subtropical Agriculture, Chinese Academy of Sciences;

Hui HUANG and Youshao WANG, the South China Sea Institute of Oceanology, Chinese Academy of Sciences;

Xinrong LI, Wenzhi ZHAO and Xueyong ZHAO, the Cold and Arid Regions Environmental and Engineering Research Institute, Chinese Academy of Sciences;

Luxiang LIN and Yiping ZHANG, Xishuangbanna Tropical Botanical Garden, Chinese Academy of Sciences;

Yan LI, Fanjiang ZENG and Chengyi ZHAO, Xinjiang Institute of Ecology and Geography, Chinese Academy of Sciences;

Zhu OUYANG, Huimin WANG and Yangjian ZHANG, the Institute of Geographic Sciences and Natural Resources Research, Chinese Academy of Sciences;

Boqiang QIN, the Nanjing Institute of Geography and Limnology, Chinese Academy of Sciences;

Weijun SHEN and Guoyi ZHOU, the South China Botanical Garden, Chinese Academy of Sciences;

Yanjun SHEN, the Institute of Genetics and Developmental Biology, Chinese Academy of Sciences;

Song SUN, the Institute of Oceanology, Chinese Academy of Sciences;

Genxu WANG and Bo ZHU, the Institute of Mountain Hazards and Environment, Chinese Academy of Sciences;

Ping XIE, the Institute of Hydrobiology, Chinese Academy of Sciences;

Fawei ZHANG, the Northwest Institute of Plateau Biology, Chinese Academy of Sciences.

REFERENCES

Arola, A., K. Lakkala, A. Bais, J. Kaurola, C. Meleti, and P. Taalas, 2003: Factors affecting short- and long-term changes of spectral UV irradiance at two European stations. *J. Geophys. Res.: Atmos.*, **108**(D17), 4549, doi: 10.1029/2003JD003447.

Bais, A. F., C. S. Zerefos, C. Meleti, I. C. Ziomas, and K. Tourpali, 1993: Spectral measurements of solar UVB radiation and its relations to total ozone, SO_2, and clouds. *J. Geophys. Res.: Atmos.*, **98**(D3), 5199–5204, doi: 10.1029/92JD02904.

Bernhard, G., C. R. Booth, J. C. Ehramjian, R. Stone, and E. G. Dutton, 2007: Ultraviolet and visible radiation at Barrow, Alaska: Climatology and influencing factors on the basis of version 2 National Science Foundation network data. *J. Geophys. Res.: Atmos.*, **112**(D9), D09101, doi: 10.1029/2006JD007865.

Calbó, J., D. Pagès, and J. A. González, 2005: Empirical studies of cloud effects on UV radiation: A review. *Rev. Geophys.*, **43**(2), RG2002, doi: 10.1029/2004RG000155.

den Outer, P. N., H. Slaper, J. Kaurola, A., Lindfors, A. Kazantzidis, A. F. Bais, U. Feister, J. Junk, M. Janouch, and W. Josefsson, 2010: Reconstructing of erythemal ultraviolet radiation levels in Europe for the past 4 decades. J. Geophys. Res.: Atmos., 115(D10), D10102, doi: 10.1029/2009JD012827.

Ferrero, E., M. Eöry, G. Ferreyra, I. Schloss, H. Zagarese, M. Vernet, and F. Momo, 2006: Vertical mixing and ecological effects of ultraviolet radiation in planktonic communities. Photochemistry and Photobiology, 82(4), 898–902, doi: 10.1562/2005-11-23-RA-736.

Foyo-Moreno, I., J. Vida, and L. Alados-Arboledas, 1999: A simple all weather model to estimate ultraviolet solar radiation (290–385 nm). *J. Appl. Meteor.*, **38**(7), 1020–1026, doi: 10.1175/1520-0450(1999)038<1020:ASAWMT>2.0.CO;2.

Gueymard, C. A., 2004: The sun's total and spectral irradiance for solar energy applications and solar radiation models. *Solar Energy*, **76**(4), 423–453, doi: 10.1016/j.solener.2003.08.039.

Hu, B., Y. S. Wang, and G. R. Liu, 2007: Ultraviolet radiation spatio-temporal characteristics derived from the ground-based measurements taken in China. *Atmos. Environ.*, **41**(27), 5707–5718, doi: 10.1016/j.atmosenv.2007.02.044.

Hu, B., Y. S. Wang, and G. R. Liu, 2010: Variation characteristics of ultraviolet radiation derived from measurement and reconstruction in Beijing, China. *Tellus B*, **62**(2), 100–108, doi: 10.1111/j.1600-0889.2010.00452.x.

Huang, M. L., H. Jiang, W. M. Ju, and Z. Y. Xiao, 2011: Ultraviolet radiation over two lakes in the middle and lower reaches of the Yangtze River, China: An innovative model for UV estimation. *Terrestrial, Atmospheric and Oceanic Sciences*, **22**(5), 491–506, doi: 10.3319/TAO.2011.05.02.01(A).

Kerr, J. B., and V. E. Fioletov, 2008: Surface ultraviolet radiation. *Atmos.-Ocean*, **46**(1), 159–184, doi: 10.3137/ao.460108.

Liu, H., B. Hu, L. Zhang, Y. S. Wang, and P. F. Tian, 2016: Spatiotemporal characteristics of ultraviolet radiation in recent 54 years from measurements and reconstructions over the Tibetan Plateau. *J. Geophys. Res.: Atmos.*, **121**(13), 7673–7690, doi: 10.1002/2015JD024378.

Long, C. N., and T. P. Ackerman, 2000: Identification of clear skies from broadband pyranometer measurements and calculation of downwelling shortwave cloud effects. *J. Geophys. Res.: Atmos.*, **105**(D12), 15 609–15 626, doi: 10.1029/2000JD900077.

Mayer, B., and A. Kylling, 2005: Technical note: The libRadtran software package for radiative transfer calculations - description and examples of use. *Atmospheric Chemistry and Physics*, **5**, 1855–1877, doi: 10.5194/acp-5-1855-2005.

Podstawczyńska, A., 2010: UV and global solar radiation in Łódź, Central Poland. *International Journal of Climatology*, **30**(1), 1–10, doi: 10.1002/joc.1864.

Schwander, H., P. Koepke, and A. Ruggaber, 1997: Uncertainties in modeled UV irradiances due to limited accuracy and availability of input data. *J. Geophys. Res.: Atmos.*, **102**(D8), 9419–9429, doi: 10.1029/97JD00244.

Tang, W. J., K. Yang, J. Qin, C. C. K. Cheng, and J. He, 2011: Solar radiation trend across China in recent decades: A revisit with quality-controlled data. *Atmospheric Chemistry and Physics*, **11**, 393–406, doi: 10.5194/acp-11-393-2011.

Tang, W. J., J. Qin, K. Yang, X. L. Niu, X. T. Zhang, Y. Yu, and X. D. Zhu, 2013a: Reconstruction of daily photosynthetically active radiation and its trends over China. *J. Geophys. Res.: Atmos.*, **118**(23), 13 292–13 302, doi: 10.1002/2013JD020527.

Tang, W. J., K. Yang, J. Qin, and M. Min, 2013b: Development of a 50-year daily surface solar radiation dataset over China. *Science China Earth Sciences*, **56**(9), 1555–1565, doi: 10.1007/s11430-012-4542-9.

Thomas, P., A. Swaminathan, and R. M. Lucas, 2012: Climate change and health with an emphasis on interactions with ultraviolet radiation: A review. *Global Change Biology*, **18**(8), 2392–2405, doi: 10.1111/j.1365-2486.2012.02706.x.

Wang, L. C., W. Gong, Y. Y. Ma, B. Hu, W. L. Wang, and M. Zhang, 2013: Analysis of ultraviolet radiation in Central China from observation and estimation. *Energy*, **59**, 764–774, doi: 10.1016/j.energy.2013.07.017.

Wei, K., W. Chen, and R. H. Huang, 2006: Long-term changes of the ultraviolet radiation in China and its relationship with total ozone and precipitation. *Adv. Atmos. Sci.*, **23**(5), 700–710, doi: 10.1007/s00376-006-0700-3.

Williamson, C. E., and Coauthors, 2014: Solar ultraviolet radiation in a changing climate. *Nature Climate Change*, **4**(6), 434–441, doi: 10.1038/nclimate2225.

Xia, X., Z. Li, P. Wang, M. Cribb, H. Chen, and Y. Zhao, 2008: Analysis of relationships between ultraviolet radiation (295–385 nm) and aerosols as well as shortwave radiation in North China Plain. *Annales Geophysicae*, **26**(7), 2043–2052, doi: 10.5194/angeo-26-2043-2008.

Yang, K., G. W. Huang, and N. Tamai, 2001: A hybrid model for estimating global solar radiation. *Solar Energy*, **70**(1), 13–22, doi: 10.1016/S0038-092X(00)00121-3.

Yang, K., T. Koike, and B. S. Ye, 2006: Improving estimation of hourly, daily, and monthly solar radiation by importing global data sets. *Agricultural and Forest Meteorology*, **137**(1–2), 43–55, doi: 10.1016/j.agrformet.2006.02.001.